(REFEREED RESEARCH)

EXPERIMENTAL STUDY AND NUMERICAL SIMULATION OF THE AIR PERMEABILITY OF SYSTEMS OF WOVEN MACROSTRUCTURES

R. A. ANGELOVA[1*], E. GEORGIEVA[1], M. KYOSOV[2] and P. STANKOV[3]

[1] Department of Textiles, Technical University of Sofia, Sofia 1000, Bulgaria
[2] Department of Hydroaerodynamics nd Hydraulic Machines, Technical University of Sofia, Sofia 1000, Bulgaria
[3] *Centre for Research and Design in Human Comfort, Energy and Environment (CERDECEN), Technical University of Sofia, Sofia 1000, Bulgaria*

Received: 18.05.2016 Accepted: 19.10. 2016

ABSTRACT

The transfer of air through systems of two woven macrostructure is studied experimentally and numerically. The influence of the properties of the layers, the array of the layering and the angle between the layers are analyzed from the point of view of the air permeability of the system. Results from the 3D simulation of the air permeability in through-thickness direction of systems of two consecutive woven macrostructures are also presented. An approach, based on modelling of the woven macrostructure as a jet system, is used to numerically predict the air transfer. Control volume method, Reynolds Averaged Navier-Stokes equations and Fluent CFD software package are applied for the simulation. The numerical results are compared with the experiments and the verification shows that the method can be successfully applied for simulation of the air transfer through multilayer systems.

Keywords: Air pPermeability; System of layers; Woven macrostructures; Computational Fluid Dynamics.

Corresponding Author: R. A. Angelova, radost@tu-sofia.bg

INTRODUCTION

Air permeability (AP) is one of the important features of porous textile macrostructures, applied in to clothing, as filterration media, geo-textiles, etc. The hierarchical structure of woven textiles makes the process of air transfer through them quite complex: the air flows through both the macrostructure (pores between the threads) and mesostructure (the voids between the fibers, spun into threads) [1]. AP is highly dependent on the shape and size of the pores in the macrostructure, which are strongly influenced by the characteristics of the woven macrostructures: the type of fibers, weave, warp and weft density, etc. [2]. Several studies have been dedicated to theoretical [3-5] or experimental investigation of the porosity of woven macrostructures [6-8]. The AP of single woven macrostructures has been also studied by a number of authors [2, 9-12]. Air permeability has been used even to predict thermal conductivity of non-wovens [13].

Besides the experimental studies, modeling of AP of textile macrostructures has been also performed [1, 3, 11, 14-17]. The transfer of fluid through a single pore of a monofilament woven fabric was simulated [17]. Latis–Boltzmann method was applied to predict the transport of fluids in a polyfilament macrostructures [11]. The AP of composite structures was predicted using a specialized CFD code [18]. Recently, the AP of woven fabrics was simulated using artificial neural networks [19]. The same technique was used to predict the permeability of single jersey fabrics [20]. Statistical modeling was applied to for the AP of cotton/polyester knitted fabrics [21]. The permeability of woven fabrics under specific out-of-plane deformation was modeled analytically [22].

There are several applications, when two or more layers from one and the same or different macrostructures are used. The system of layers has a different permeability from the compound single layers. The last affects the thermal insulation of clothing ensembles, for example, or the thermophysiological comfort of bedridden people [23]. Main reasons for that are the change in the porosity of the single layers and the layer (or layers) of air, retained between the textile macrostructures. However, the porosity of the system of layers cannot be calculated, as it is done in the case of single layers. Therefore it is difficult to estimate how the

porosity of the system has changed, on the first place, and how the transfer of air is affected, on the second.

The literature survey has shown that the problem of air permeability of a multilayer system of woven macrostructures has not been a topic of systematic research. Therefore the present study aimed to determine experimentally and to simulate numerically the through-thickness air transfer through systems of two woven macrostructures. The influence of the characteristics of the macrostructures and the lay-up of the single layers on the AP of the system was studied. Different lay-up settings and positioning of the two layers (angle between warp and weft threads) were tested, which has not been reported in the literature. 3D simulation of the air permeability in through-thickness direction of two consecutive woven macrostructures was also performed. An approach, based on modelling of the flow through the woven macrostructure as a jet system, was applied, using the control volume method and Fluent CFD software package. The numerical results were compared with the experimental data and the verification showed that the method could be successfully applied for simulation of the air transfer through multilayer systems.

MATERIALS AND METHODS

Experimental measurements

Fourteen cotton woven macrostructures (called “single layers” or SL) were involved in the study. They were selected to be with a wide range of mass per unit area (from 63 to 235 g/m^2) and thickness (from 0.39 to 0.71 mm). were selected for preparation of the system of layers with a range of mass per unit area from 63 to 235 g/m^2.

Their characteristics were experimentally determined after 24-hours conditioning (22^{o}C, 65% RH). The mass per unit area was measured in accordance with ISO 3801:1977 2011 [24] and the thickness – following EN ISO 5084:201302 [25]. ISO 7211-2:20101984 [26] was used to determine warp and weft densities. The mean pore size of the macrostructures was measured with Optika DM-15 microscope and built-in digital camera (1600x1200 pixels), following the described methodology described in [27].

Table 1 shows the basic characteristics of the single layers and woven macrostructures, used for the composition of 77 two layer systems (TLS). Fig.ure 1 presents the microscopic view (4x-enlargements) of the single macrostructureslayers.

The single layers were used for composing 77 two-layer systems (TLSs). A different code was given to each system, showing the top and the bottom layer: for example the TLS2-4 system was composed by SL2 as a top layer and SL4 as a bottom layer, while the TLS4-2 system was composed by SL4 as a top layer and SL2 as a bottom layer.

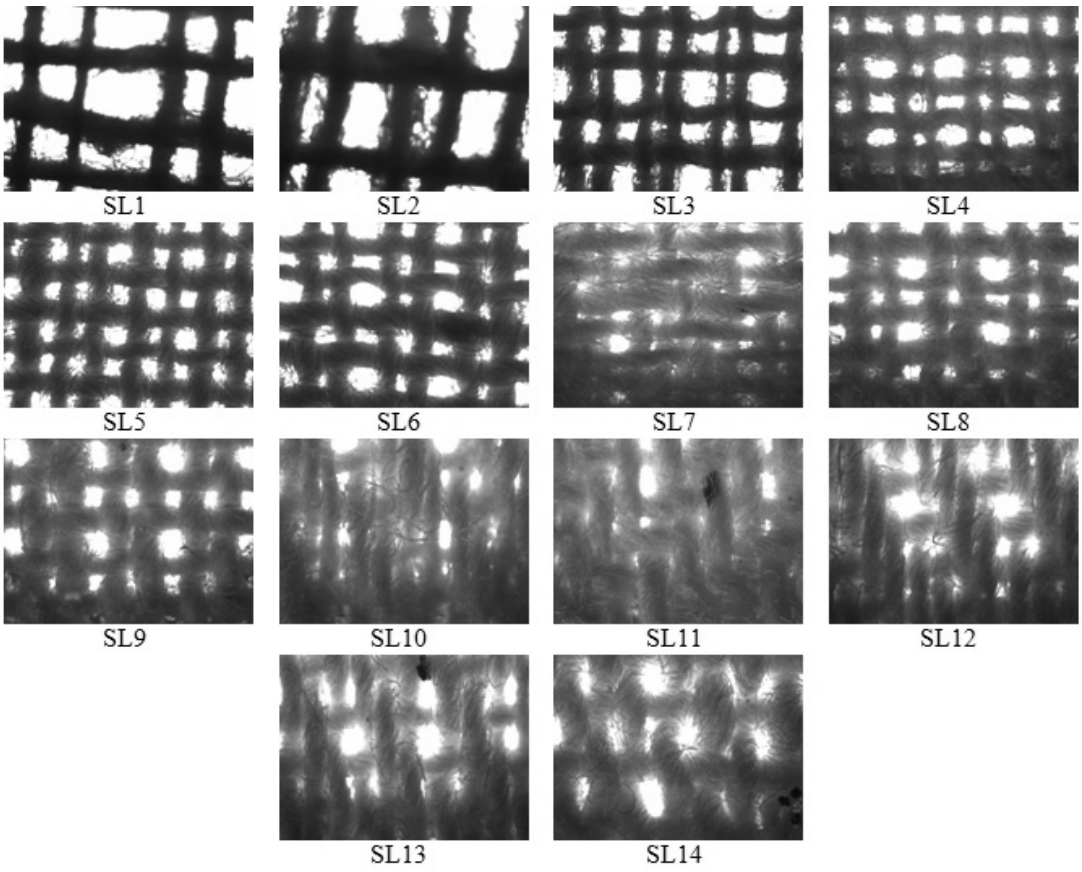

Fig. 1. Microscopic view of the selected woven macrostructures (4x enlargement)

Table 1. Properties of the selected woven macrostructures

Sample	Mass per unit area, g/m^2	Warp density, dm^{-1}	Weft density, dm^{-1}	Warp yarn linear density, tex	Weft yarns linear density, tex	Mean pore area, mm^2	Thickness , mm	Weave
SL1	63	142	166	20	20	0.243	0,43	plain
SL2	89	176	124	28	28	0.255	0,45	plain
SL3	118	272	218	20	25	0.031	0,39	plain
SL4	133	284	294	20	20	0.040	0,39	plain
SL5	138	270	266	25	25	0.024	0,41	plain
SL6	157	234	254	30	30	0.046	0,47	plain
SL7	184	383	338	28	28	0.063	0,68	twill 2/1
SL8	197	252	260	36	36	0.029	0,48	plain
SL9	201	258	238	36	36	0.038	0,49	plain
SL10	202	386	226	30	36	0.024	0,71	twill 3/1
SL11	206	324	254	40	25	0.014	0,64	twill 2/2
SL12	212	402	240	30	40	0.031	0,71	twill 3/1
SL13	219	376	216	36	36	0.023	0,65	twill 2/1
SL14	235	267	166	50	50	0.024	0,62	plain

The transfer of air through TLSs was measured (20 measurements per a TLS) in accordance with EN ISO 9237:20111999, with a FF-12 apparatus of Metrimpex [28]: a 10 cm^2 measurement area and 100 Pa pressure gradient, applied on both sides of the specimen.

The following problems aimed to be analyzed:

- The effect of the lay-up: 3 macrostructures with different characteristics, but one and the same weave: SL4, SL9 and SL14, were used as first (top) layer of the system, while all other samples, composing the second (bottom) layer of the system, were kept constant.
- The effect of the positioning: 3 different angles between the warp threads of the top and the bottom macrostructures were applied: 0^o (coincidence of the warp threads of the two layers); 45^o and 90^o (the warp threads of the top layer coincided with the weft threads of the bottom layer).

Numerical simulation

Four of the layers (SL 2, SL4, SL6 and SL10) were used for preparing virtual models and performing numerical simulation of the transfer of air through a two layers system (TLS).

The numerical simulation of the air transfer through TLS was baseds on the jet-system theory. The method was successfully applied and verified in previous works for single woven macrostructures [1, 3] and also applied for knitted fabrics [29]. The basic idea of the method is to present the pores of the woven macrostructure as jet openings, which form an in-corridor ordered jet system. The air, which passes in through-thickness direction of the macrostructure, flows predominantly through the pores, i.e. the system of jets.

It was proven experimentally that in this type of jet systems every single jet is representative for the whole system, if it is surrounded by 8 other jets [30]. The jets that surround the "central jet" perform the role of boundary conditions, as they influence the development of the central jet downstream. Figure 2 presents the approach, using the example of SL4: the macroscopic view of the sample (Fig. 2a) and the approximation to a 3x3 in-corridor ordered jet-system (Fig. 2b) that involves 9 pores (3x3) and 16 threads (4x4).

To approximate the complex woven macrostructure to a jet system, some reasonable assumptions were made: * The thread's diameter was taken as a constant; * The pore area was used to calculate the average side of the square pore opening (jet opening); *It was assumed that the thickness of the SL reflects the weave pattern.

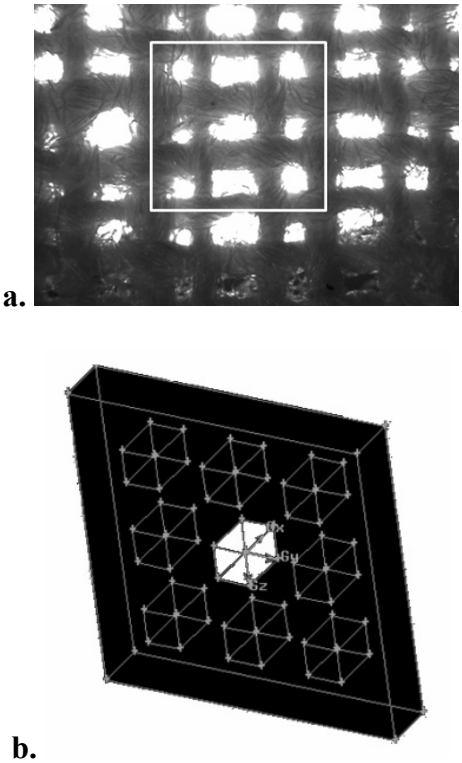

Fig. 2. Representation of the woven macrostructure as a jet system: a. Microscopic view of the woven macrostructure; b. Part of the numerical grid – the in-corridor jet systems with the highlighted central pore

The simulation of the air transfer through the woven macrostructures was based on Reynolds Averaged Navier-Stokes (RANS) equations plus the continuity equation.

A standard $k-\varepsilon$ turbulent model was used to close the system, adding additional transport equations for the turbulent kinetic energy k and its dissipation rate ε.

The geometry of each of the woven structures was built with GAMBIT pre-processor of FLUENT CFD software package, used for the simulations. A pressure difference of 100 Pa was set on the two sides of the samples (200 Pa at the domain inlet and 100 Pa at the domain outlet), so as to repeat the conditions of the experimental measurement of the air transfer through the woven macrostructures. Symmetrical boundaries were set at the surrounding walls of the domain. The solver was set-up as pressure based and implicit, over a 3D space.

The first SL was immersed in a pipe-like domain: 3 mm after the inlet and 8 mm before the outlet. The second (bottom) SL was placed at a distance of 0.5 mm after the first (top) layer. A hybrid grid of tetrahedrons (between the samples) and hexahedrons (in the rest of the domain) was applied. After performing a grid independence tests a hybrid grid was chosen with a number of cells, faces and nodes, described in Table 2 together with the simulated cases. Figure 3 shows one of the virtual models and the grid, for the TSL4-2.

RESULTS AND DISCUSSIONS

Results from the Experimental Measurements

The measured flow rate through the systems of layers was used to calculate the air permeability, namely:

$$AP = \frac{Q}{A} \quad (1)$$

where AP denotes the air permeability, m/s, Q is the measured flow rate through the sample, m^3/s, and A is the area of the sample, m^2.

Figures 4-6 present the results for the AP of system of layers, when the top SL was changed, namely SL4 (Fig. 4), SL9 (Fig. 5) and SL14 (Fig. 6). The weaves of the three macrostructures were one and the same, to avoid the possible influence of the yarns interlacing on the flow resistance. However, the three single layers differ in terms of their thickness and mass per unit area (Table 1).

Table 2. Simulated cases

Case	Code	First layer	Second layer	Number of Cells	Number of Faces	Number of Nodes
1	TLS2-4	SL2	SL4	134350	391110	125501
2	TLS4-2	SL4	SL2	128318	373014	119469
3	TLS4-6	SL4	SL6	71799	211721	69636
4	TLS4-10	SL46	SL104	425966	1071864	219064
5	TLS6-4	SL6	SL4	68103	200633	65940

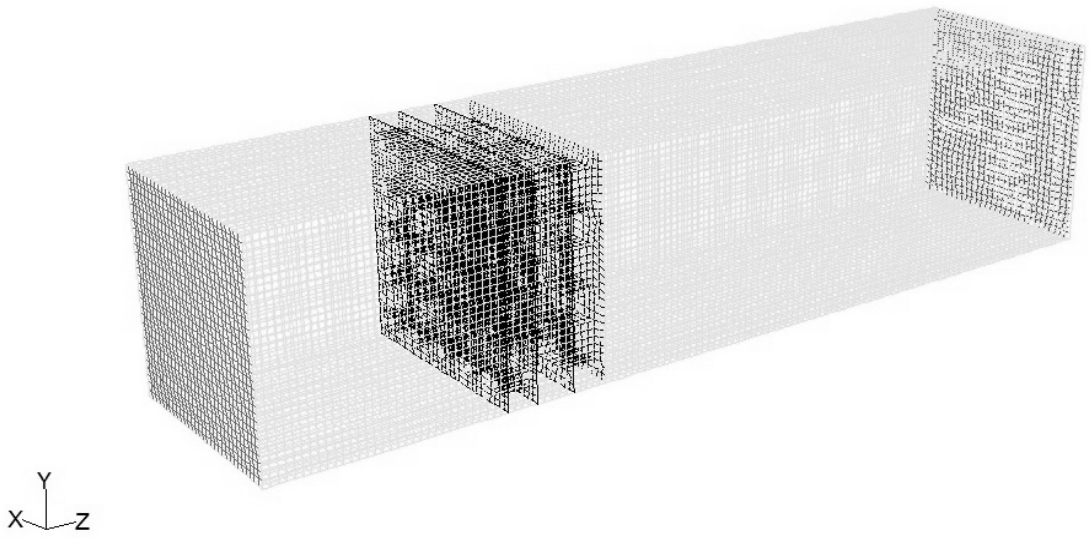

Fig. 3. Numerical domain and a grid for TSL4-2

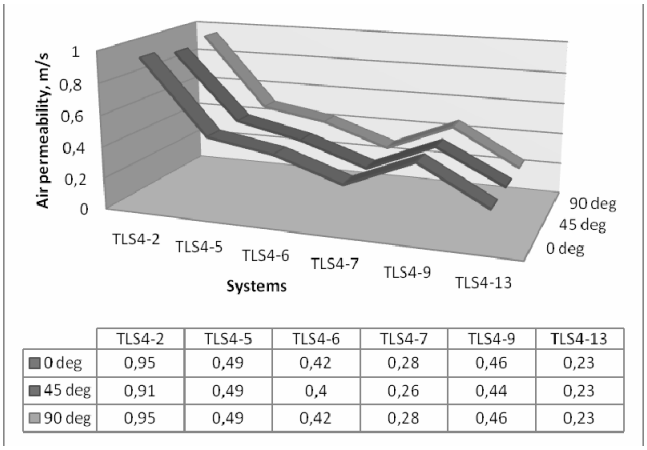

	TLS4-2	TLS4-5	TLS4-6	TLS4-7	TLS4-9	TLS4-13
0 deg	0,95	0,49	0,42	0,28	0,46	0,23
45 deg	0,91	0,49	0,4	0,26	0,44	0,23
90 deg	0,95	0,49	0,42	0,28	0,46	0,23

Fig. 4. Air permeability of TLSs with SL4 as a top layer

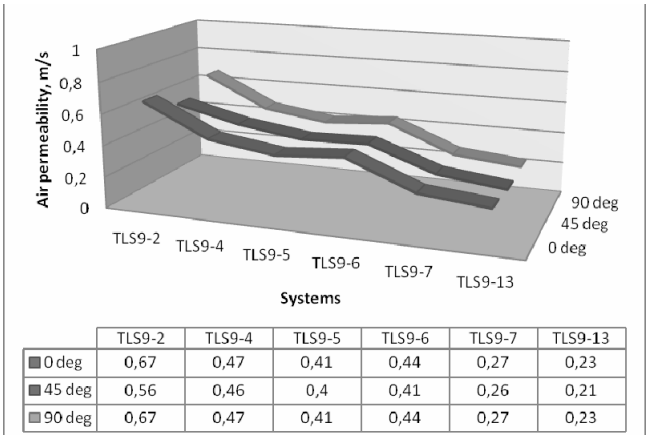

	TLS9-2	TLS9-4	TLS9-5	TLS9-6	TLS9-7	TLS9-13
0 deg	0,67	0,47	0,41	0,44	0,27	0,23
45 deg	0,56	0,46	0,4	0,41	0,26	0,21
90 deg	0,67	0,47	0,41	0,44	0,27	0,23

Fig. 5. Air permeability of TLSs with SL9 as a top layer

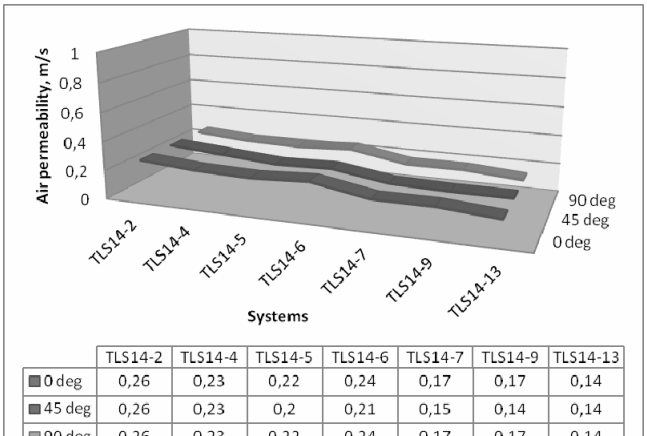

	TLS14-2	TLS14-4	TLS14-5	TLS14-6	TLS14-7	TLS14-9	TLS14-13
0 deg	0,26	0,23	0,22	0,24	0,17	0,17	0,14
45 deg	0,26	0,23	0,2	0,21	0,15	0,14	0,14
90 deg	0,26	0,23	0,22	0,24	0,17	0,17	0,14

Fig. 6. Air permeability of TLSs with SL14 as a top layer

To visualize the difference in the air permeability of the TLS one and the same values of the Y-axis were used in the graphs on Figs. 4-6. The highest values of the air flow rate, transferred through TLS, were obtained with SL4, placed as a top layer (Fig. 4). The lowest was the air permeability of TLSs with SL14 as a top layer (Fig. 6). For example, when SL5 was used as a bottom layer, the AP of the system TLS4-5-0 (SL4 top layer) was 0.49 m/s, while for the systems TLS9-5-0 (SL9 top layer) and TLS14-5-0 (SL14 top layer) the average values were 0.41 m/s and 0.22 m/s, respectively.

At the same time, the air permeability of some of the systems with SL4 (Fig. 4) and SL9 (Fig. 5) as a top layer, were very similar: for TSL4-6 and TSL9-6, for TSL4-7 and TSL9-7, and for TSL4-13 and TSL9-13. A possible explanation of these results can be found in the way the air is transferred in through-thickness direction of a woven macrostructure [27]. Part of the flow moves through the pores of the macrostructure (between warp and weft threads), and part of the flow, though much lesser, passes through the pores of the mesostructure (between the fibers, forming the threads). Using computer simulation, it was found [27] that less than 5% of the total air flow rate passes through the mesostructure [27]. In the present case not only the top, but also the bottom layer influences the air permeability of TLS. When SL2 and SL4 macrostructures were used as bottom layers, their higher porosity allowed easier transport of the air through the system. In the case of SL6, SL7 and SL13, used as bottom layers, the influence of the top layer was much higher. Being different in thickness and mass per unit area, SL4 and SL9 macrostructures have very similar mean pore area (pores of the macrostructure): 0.040 mm^2 and 0.038 mm^2, respectively. Due to the low percentage of the total flow rate, which can pass through the pores of the mesostructure, obviously the similar pore area of the top layers leaded to a similar air permeability of TSLs.

An important analysis can be also made comparing the results for TLS4-9 (Fig. 4) and TLS9-4 (Fig. 5). The difference between the systems is that SL4 and SL9 change their position as top and bottom layers (Table 2). Evidence is shown in the graphs that the AP of all three systems, where SL94 is used as a top layer and SL49 – as a bottom layer – is higher than the AP of the three systems, where the order of layering is reversed. The difference between the mean values is less than 3% for the systems, with an angle of 0^o and 90^o between warp and weft threads, and 5% for the systems, layered at 45^o. An explanation can be found in the difference, though a small one, between the pore area of SL4 and SL9. The flow rate through the pores of SL4 is higher than through the pores of SL9 due to the higher voids between the threads, thus provoking greater air permeability of the system higher flow rate is transferred when the more porous layer is at the bottom side.

through the pores of the bottom layer (SL9). On the contrary, when SL9 is the top layer, smaller flow rate passes through its smaller pores and the total AP of the system is lower.

Figures 7 and 8 are useful for the analysis of the effect of the angle of positioning of between the warp threads of both top and bottom layers. Two groups of exemplary results are presented: when the top layer changes (SL4, SL9 and SL14), while the bottom layers is SL2 (Fig. 7), and the same top layers combined with SL7 as a bottom layer (Fig. 8).

The angle of positioning between the two layers in the TLS has not influenced quite much the transfer of air flow through them. In almost all cases there is no difference between the cases with 0^o and 90^o layering. Only the rotation of the bottom layer on 45^o toward the top layer

decreased the air permeability in some of the cases, i.e. by 4% in the case of TLS4-2 (45°) compared to TLS4-2 (0°) or by 16% in the case of TLS9-2 (45°) compared to TLS9-2 (0°). In some cases the rotation of the two layers did not have an effect on the air permeability.

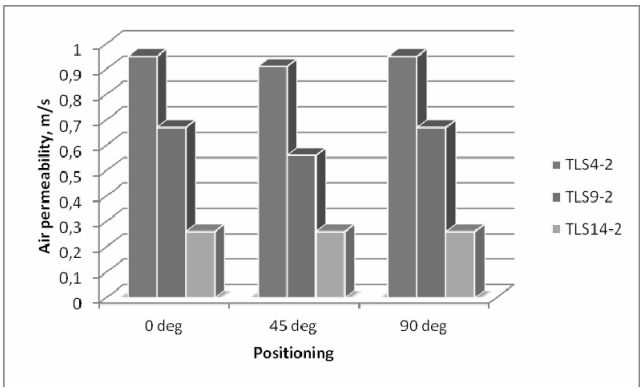

Fig. 7. Air permeability of TLSs with SL24 as a top bottom layer

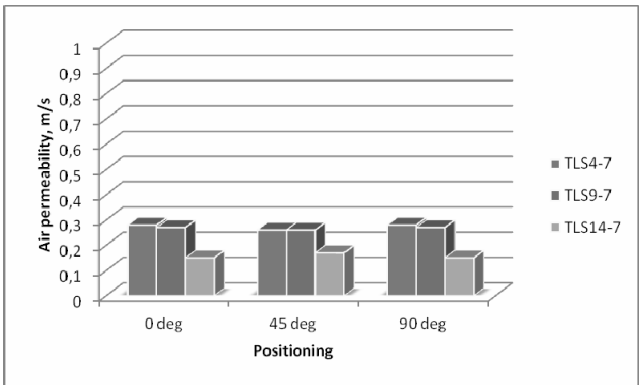

Fig. 8. Air permeability of TLSs with SL79 as a top bottom layer

Results from the Numerical Simulation

Figure 9 visualizes the velocity field for TLS4-2, composed by of a sample with low porosity (SL4) as a top layer and a sample with high porosity (SL24) as a bottom layer and a sample with low porosity (SL4). The velocity of the developed flow (a steady state flow) after the samples has the meaning of air permeability, obtained as a quotient between the flow rate through the sample Q, m^3/s, and the area of the sample A, m^2. For comparison, it is also shown the velocity field of TLS4-6: (a system, composed of layers with similar values of warp and weft density and pore area) is also shown in – Fig. 10. Obviously, when samples with different porosity compose the system of two layers, part of the pores of the first layer are closed by the threads of the second layer, but this is the same in the reality. The predicted air permeability of TLS4-2 is 0.85 m/s (Fig. 9), while for TLS4-6 is 0.38 m/s (Fig. 10), due to the smaller pores between the threads of SL4 and SL6.

Figures 11 and 12 compare the centerline velocity decay of the air flow, transferred through TLS4-6 and TLS6-4, where the same single layers are used, but placed on a reverse order. Figures 13 and 14 present the static pressure of the flow through the same systems.

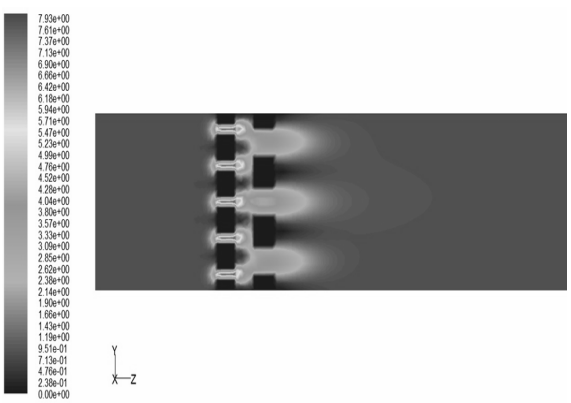

Fig. 9. Visualization of the air transfer through TLS4-2: velocity field (m/s).

Fig. 10. Visualization of the air transfer through TLS4-6: velocity field (m/s)

The centerline velocity decay allows assessing the influence of the lay-up of the system. Theoretically, the air permeability is a cumulative property of the textiles and the lay-up order of the single textiles in the system would not affect the total flow rate, passed through the system. The results obtained have shown that the order of the layers has an influence on the flow development, as the second sample changes the boundary air layer between the two textiles in the system, as it can be seen from Figures 11 – 14. Though the flow development through the two systems is quite different, the predicted air permeability is similar: 0.38 m/s for TLS4-6 (Fig. 11) and 0.4 m/s for TLS6-4 (Fig. 12).

Verification of the Numerical Results for the Air Permeability of TLS

The comparison between the numerical and experimental results is performed for three of the TLSs, as shown in Fig. 15: TLS4-2, TLS4-6 and TLS4-10. The verification of the numerical allows to conclude that all numerical results are a bit smaller than the experimental readings. The calculation of the error (calculated as the difference between the experimental and numerical values, divided into the experimental values) shows that the error is less than 10% for TLS4-2 and TLS4-6, and 15% for TLS4-10, which is quite a good coincidenceconcordance, having in mind the simplifications made for in the simulation of the woven macrostructures.

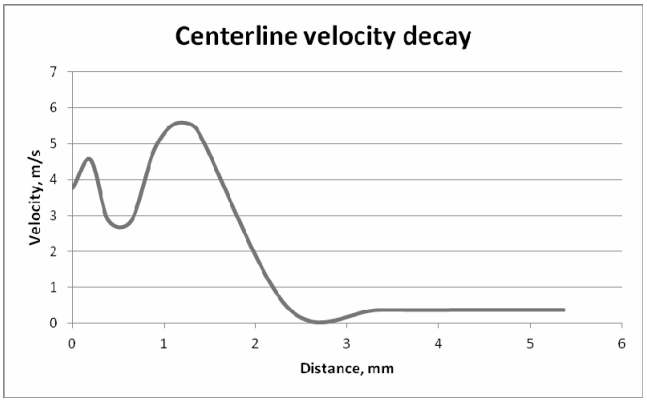

Fig. 11. Centerline velocity decay of the air flow through TLS4-6

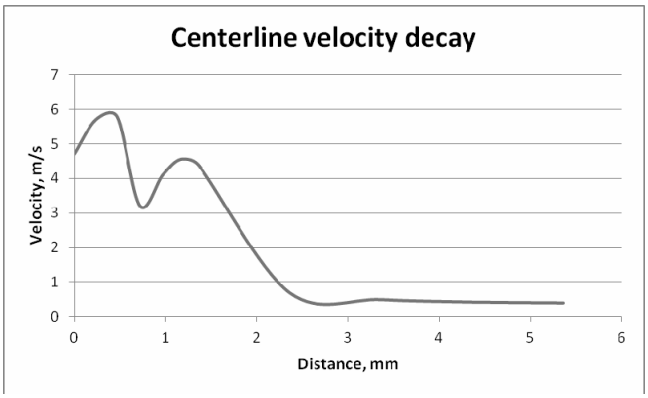

Fig. 12. Centerline velocity decay of the air flow through TLS6-4

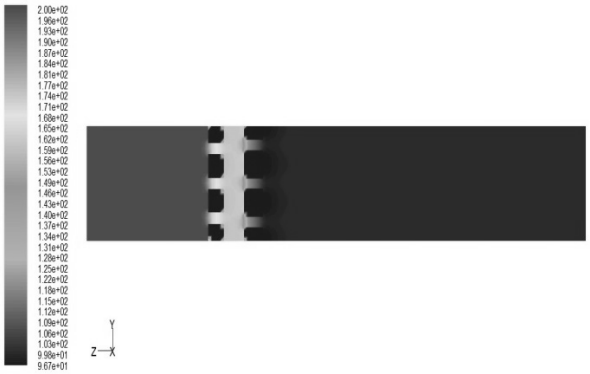

Fig. 13. Static pressure (Pa) of the air flow through TLS4-6

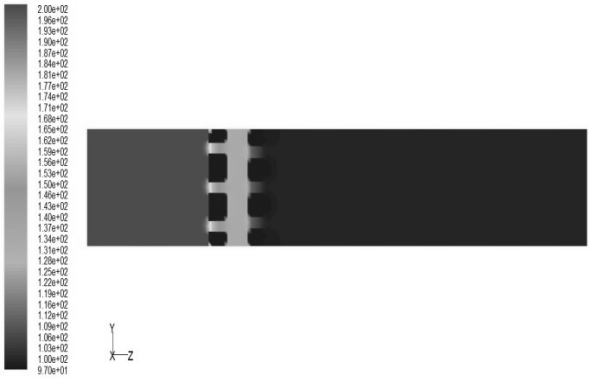

Fig. 14. Static pressure (Pa) of the air flow through TLS6-4

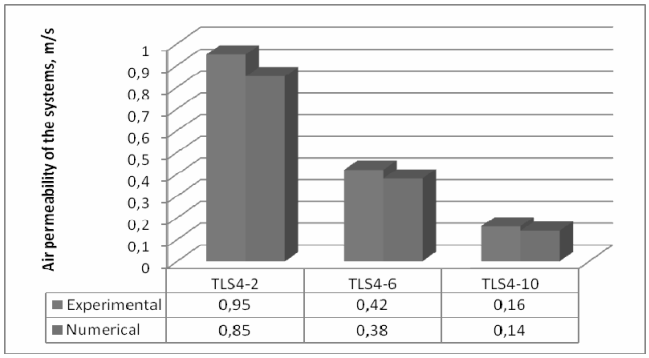

Fig. 15. Comparison between experimental and numerical results for the air permeability

The results are in a very good correlation with the established tendency in [27] that the predicted air permeability of tightly woven fabrics differs more from the experimental measurements, if compared with fabrics with greater porosity. An explanation is that the applied method for simulation of the transfer of air through a system of layers does not include the transfer of air through the pores of the mesostructure (pores between the fibers in the threads). When the sample is less porous, greater part of the fluid is transferred through the pores of the mesostructure. However, it was found that for single layers this value is approximately 2% [27].

The lower predicted values, compared to the experimental measurements, show that there is a part of the air flow, which is transferred not only through the pores between the threads, but also through the pores between the yarns in the threads. Our future work will be dedicated to an in-depth numerical investigation of this problem.

CONCLUSIONS

Results from experimental measurements and numerical prediction of the air permeability of systems of woven structures were presented.

It was found that the increment of thickness and mass per unit area of the TLSs decreases their ability to transfer air in through thickness direction. The highest values of the air permeability were obtained when a thinner layer with lower mass per unit area was placed as a top layer.

The analysis performed has shown that the air permeability of the TLS changes when the layering array changes, but the established difference is between 0 and 5%. The angle of positioning between the two layers in the TLS has not a big influence on the transfer of flow through them. Only the rotation of the bottom layer on 45^{o} toward the top layer decreased the air permeability by 4 to 16%.

The results from the CFD simulation of the air transfer in through-thickness direction of a single layer woven macrostructures and systems of two consecutive woven macrostructures showed the importance of the properties of the SL and the TLS for the flow parameters after the textile barrier. The modeling approach, based on presentation of the woven macrostructure as a jet system was verified for a system of two layers and a good coincidence between the numerical and experimental results was ascertained.

REFERENCES

1. Angelova, R.A., Stankov, P., Simova, I., and Aragon I., Three Dimensional Simulation ofAir Permeability of Single Layer Woven Structures, Cent. Eur. J. Eng. 1 (4), 430-435 (2011).
2. Ogulata R. T. (2006). Air permeability of woven fabrics. J Textile Apparel, Technology and Management. 5 (2), 1-10.
3. Angelova R. A., P. Stankov, I. Simova, and M. Kyosov (2013). Computational Modeling and Experimental Validation of the Air Permeability of Woven Structures on the Basis of Simulation of Jet Systems. Text. Res. J. 83 (18), 1887-1895.
4. Peirce F. T. and F. T. Womersley (1978). Cloth Geometry. Manchester, England: Text. Institute.
5. Seyam A. and A. El-Shiekh (1993). Mechanics of Woven Fabrics. Text. Res. J. 63 (2), 371-378.
6. Dubrovski P. D. and M. Brezocnik (2002). Using Genetic Programming to Predict the Macroporosity of Woven Cotton Fabrics. Text. Res. J. 72 (3), 187-194.
7. Jakšic D. and N. Jakšic (2007). Assessment of Porosity of Flat Textile Fabrics. Text. Res. J. 77 (2), 105-110.
8. Zupin Z., A. Hladnik and K. Dimitrovski (2012). Prediction of One-Layer Woven Fabrics Air Permeability Using Porosity Parameters. Text. Res. J. 82 (1), 117-128.
9. Fatahi, II., and Alamdar, Y. A., "Assessment of the Relationship between Air Permeability of Woven Fabrics and Its Mechanical Properties", Fib Text East Europe. 18 (6), 68-71, (2010).
10. Havlova, M., "Influence of Vertical Porosity on Woven Fabric Air Permeability", 7th International Conference - TEXSCI 2010, Liberec, Czech Republic, (2010).
11. Nabovati A., E. W. Llewellin and A. C. M. Sousa (2010). Through-thickness permeability prediction of 3D multifilament woven fabrics, Composites. Part A 41, 453-463.
12. Rief S., E. Glatt, E. Laourine, et al. (2011). Modelling and CFD-Simulation of Woven Textiles to Determine Permeability and Retention Properties. AUTEX Res J. 11, 78-83.
13. Banks-Lee, P., Mohammadi, M., and Ghadimi, P., "Utilization of Air Permeability in Predicting the Thermal Conductivity", Int. Nonwovens J. 13(2), 28-33 (2004).
14. Gooijer H., M. M. C. G. Warmoeskerken. and J. Groot Wassink (2003a). Flow Resistance of Textile Materials Part I: Monofilament Fabrics. Text. Res. J. 73(5), 437-443.
15. Gooijer H., M. M. C. G. Warmoeskerken. and J. Groot Wassink (2003b). Flow Resistance of Textile Materials Part II: Multifilament Fabrics. Text. Res. J. 73(6), 480-484.
16. Belov E. B., S. V. Lomov, I. Verpoest, T. Peters, D. Roose, R. S. Parnas, K. Hoes and H. Sol (2004). Modelling of permeability of textile reinforcements: lattice Boltzmann method, Compos Sci and Tech. 64 (7–8), 1069-1080.
17. Verleye B., M. Klitz, R. Groce, D. Roose, S. V. Lomov and I. Verpoest (2007). Computation of the permeability of textiles with experimental validation for monofilament and non crimp fabrics. Studies in Computational Intelligence, Springer.
18. Wang Q., B. Maze, H. V. Tafreshi (2007). On the pressure drop modeling of monofilament-woven fabrics. Chemical Eng. Science. 62 (17), 4817-4821.
19. Grouve, W. J. B., Akkerman, R., Loendersloot, R., and van den Berg, S. (2008), "Transverse permeability of woven fabrics", 11th ESAFORM Conference on Material Forming, April 23-25, Lyon, France, (2008).
20. Matusiak M. (2015) Application of Artificial Neural Networks to Predict the Air Permeability of Woven Fabrics. Fibers & Text. in Eastern Europe. 23 (1), 41-48.
21. Unal P., M. Üreyen, and D. Mecit (2012), Predicting Properties of Single Jersey Fabrics using Regression and ANN Models, Fibers and Polymers. 13 (1), 87-95.
22. Afzal A., T. Hussain, M. Malik, A. Rasheed, S Ahmad, A. Basit and A. Nazir (2014). Investigation and Modeling of Air Permeability of Cotton/Polyester Blended Double Layer Interlock Knitted Fabrics. Fibers and Polymers. 15 (7), 1539-1547.
23. Xiao X., A. Long and X. Zeng (2014). Through-thickness permeability modelling of woven fabric under out-of-plane deformation. J Mater Sci. 49 7563-7574.
24. Angelova R. A. (2016). Textiles and Human Thermophysiological Comfort in the Indoor Environment. CRC Press, Taylor and Francis Group, Boca Raton, FL, USA.
25. ISO 3801:2011, Textiles -– Woven fabrics -– Determination of mass per unit length and area, IOS, Switzerland.
26. EN ISO 5084:201302. Textiles -– Determination of thickness of textiles and textile products. IOS, Switzerland.
27. ISO 7211-2:20101984, Textiles -– Woven fabrics -– Construction - Methods of analysis - Part 2, IOS, Switzerland.
28. Angelova R. A. (2012). Determination of the Pore Size of Woven Structures through Image Analysis, Cent. Eur. J. Eng. 2 (1), 129-135.
29. Mezarcioz S., S. Mezarcioz, R.T. Ogulata, Prediction of the Air Permeability of Knitted Fabrics by Means of Computational Fluid Dynamics, Tekstil ve KonfeksiyonEKSTİL ve KONFEKSİYON 24(2), pp. 202-211, 2014.
30. EN ISO 9237:20111999. Textiles-Determination of permeability of fabrics to air, IOS, Switzerland.
31. Stankov P, Three dimensional turbulent flows in heat and mass transfer processes, D.Sc. Thesis, Technical University of Sofia, Bulgaria, 1998.